THE LEAKING MODE PROBLEM IN ATMOSPHERIC ACOUSTIC-GRAVITY WAVE PROPAGATION*

Wayne A. Kinney and Allan D. Pierce
Georgia Institute of Technology

SUMMARY

Previous attempts to predict the transient acoustic pressure pulse at long horizontal distances from large explosions in the atmosphere have adopted a model atmosphere bounded above by a halfspace of finite sound speed and have represented the waveform as a superposition of contributions from dispersively propagating guided modes. Certain modes at low frequencies decay exponentially (leaking modes) with increasing propagation distance. The practice up to now has been to neglect the contributions from such modes in such frequency ranges. The lower frequency cutoffs for such modes are extremely sensitive to the nature of the upper halfspace in contradiction to the reasonable supposition that energy ducted in the lower atmosphere should be insensitive to the assumed form of the upper halfspace. In the present paper the overall problem is reexamined with account taken of poles off the real axis and of branch line integrals in the general integral governing the transient waveform. Perturbation techniques are described for the computation of the imaginary ordinate of the poles and numerical studies are described for a model atmosphere terminated by a halfspace with c = 478 m/sec above 125 km. For frequencies less than 0.0125 rad/sec, the GR_1 mode, for example, is found to have a frequency dependent amplitude decay of the order of 10^{-4} nepers/km. Examples of numerically synthesized transient waveforms are exhibited with and without the inclusion of leaking modes. The inclusion of leaking modes results in waveforms with a more marked beginning rather than a low-frequency oscillating precursor of gradually increasing amplitude. Also, the revised computations indicate that waveforms invariably begin with a pressure rise, a result supported by other theoretical considerations and by experimental data.

INTRODUCTION

One of the standard mathematical problems in acoustic wave propagation is that of predicting the acoustic field at large horizontal distances from a localized source in a medium whose properties vary with height only. This problem, as well as its counterpart in electromagnetic theory, has received considerable attention in the literature (ref. 1), is reviewed extensively in various texts (refs. 2-7), and, for the most part, may be considered to be well understood.

A typical formulation of the transient propagation problem (refs. 8,9) leads (at sufficiently large horizontal distance r) to an intermediate result

*Work supported by Air Force Geophysics Laboratory

which expresses the acoustic pressure as a double Fourier integral over angular frequency ω and horizontal wave number k so that

$$p = S(r)\ \mathrm{Re}\ \{\int_0^\infty \hat{f}(\omega)e^{-i\omega t} \int_{-\infty}^{\infty} [Q/D(\omega,k)]e^{ikr}\,dk\,d\omega\}. \qquad (1)$$

Here S(r) is a geometrical spreading factor, which is $1/\sqrt{r}$ for horizontally stratified media and $1/[a_e \sin(r/a_e)]^{1/2}$ if the earth's curvature (a_e = radius of earth) is approximately taken into account. The quantity $f(\omega)$ is the Fourier transform of a time-dependent function that characterizes the source. Q is a function of receiver and source heights z_r and z_s, respectively, as well as of ω and k, and possibly of the horizontal direction of propagation if winds are included in the formulation. In any case, given z_r and z_s, Q should have no poles in the complex k-plane when ω is real and positive. The denominator $D(\omega,k)$ (which is termed the eigenmode dispersion function) may be zero for certain values $k_n(\omega)$ of k.

The k integration contour for Eq. (1) is chosen to lie along the real k-axis except where it skirts below or above poles which lie on the real axis (see Fig. 1a, where branch lines are identified by slash marks, poles are indicated by dots, and the k integration contour is marked by arrowheads that show the direction of integration). Let it suffice here to say that the placing of branch cuts and the selection of the contour must be such that the expression for the acoustic pressure dies out at long distance as long as a small amount of damping is included in the formulation. The guided-mode description in the formulation arises when the contour is deformed [permissible because of Cauchy's theorem and of Jordan's lemma (ref. 10)] to one such as is sketched in Fig. 1b. The poles indicated there above the initial contour are encircled in the counterclockwise sense, and there are contour segments which encircle (also in the counterclockwise sense) each branch cut that lies above the real axis. The integrals around each pole are evaluated by Cauchy's residue theorem so that what remains is a sum of residue terms plus branch line integrals. Each residue term is considered to correspond to a particular guided mode of propagation.

One approximation that was previously made in the guided-mode formulation was to neglect contributions from poles [i.e., the $k_n(\omega)$] which were located above the real k-axis (refs. 8,9). The thought behind this omission was that most of the contributions in the synthesis of waveforms for long propagation distances would come from poles which were on the real k-axis. Another approximation was that, for long distances, the contribution from branch line integrals could be neglected as well. Given these two approximations, the expression for the acoustic pressure in Eq. (1) can be approximated as follows:

$$p = \sum_n S(r) \int_{\omega_{Ln}}^{\omega_{Un}} A_n(\omega)\ \cos[\omega t - k_n(\omega)r + \phi_n(\omega)]\ d\omega, \qquad (2)$$

where $A_n(\omega)$ and $\phi_n(\omega)$ are defined in terms of the magnitude and phase of the residues of the integrand in Eq. (1) and the $k_n(\omega)$ are the real roots for $D(\omega,k)$ (which are numbered in some order with n = 1,2,3, etc.). It is understood that in Eq. (2), for any given n, $k_n(\omega)$ should be a continuous function of ω between the limits ω_{Ln} (lower) and ω_{Un} (upper). With this understanding, it should be possible to evaluate the resultant integral over ω approximately

by the method of stationary phase or by some numerical method.

In spite of the seeming plausibility of the above two approximations, there is a set of circumstances intrinsic to low-frequency infrasonic propagation for which they are not valid, even for distances of propagation of more than 10,000 km. It is these circumstances and their relation to the analytic synthesis of guided-mode atmospheric infrasonic waveforms that are of central interest in this discussion.

SYMBOLS FREQUENCY USED

A_{11}, A_{12}	defined in Eqs. (6)
c_T	sound speed for upper halfspace
$c(z)$	sound speed as a function of height
$D(\omega,k)$	eigenmode dispersion function defined in Eq. (5)
G	defined in Eq. (3)
GR_0, GR_1	gravitational modes
k, k_I, k_R	horizontal wave number and its imaginary and real parts, respectively
$k_n(\omega)$	ordered roots of $D(\omega,k)$
p	acoustic pressure
r	horizontal distance of propagation
R_{11}, R_{12}	[1,1] and [1,2] elements of the transmission matrix [R], respectively
t	time
v	phase velocity (ω,k)
$v^{(1)}$	complex phase velocity obtained by first iteration with Eq. (8a)
$v_a(\omega), v_b(\omega)$	roots of $R_{11}(\omega,v)$ and $R_{12}(\omega,v)$, respectively
$v_n(\omega)$	roots of $D(\omega,v)$
z	height
z_T	height of bottom of upper halfspace
α, β	derivatives of R_{11} and R_{12} with respect to v, respectively, and evaluated at v_a and v_b, respectively
ρ_o	ambient density
ω	angular frequency
ω_A, ω_B	characteristic frequencies used in Eq. (3)
(ω_L, v_L)	cutoff point in the (ω,v)-plane for a non-leaking mode.

INFRASONIC MODES

An atmospheric model that is frequently adopted in studies of infrasound is one in which the sound speed c(z) varies continuously with height z in some reasonably realistic manner up to a specified height z_T and is constant (value c_T) for all heights exceeding z_T (see Fig. 2). Should winds be included in the formulation, the wind velocities are also assumed to be constant in the upper halfspace $z > z_T$. It would seem reasonable to say that there is some choice in specifying the values for both z_T and c_T, even though the computations of such factors as Q and $D(\omega,k)$ in Eq. (1) become more lengthy with increasing z_T. Whatever the choice of z_T, it would seem reasonable to choose c_T to be $c(z_T)$ so that the sound-speed profile would then be continuous with height. Intuitively, it would also seem that if the source and receiver are both near the ground and if the energy actually reaching the receiver travels

via modes of propagation channeled primarily in the lower atmosphere, then the actual value of the integral in Eq. (1) would be somewhat insensitive to the choices of z_T and c_T. This idea, however, remains to be justified in any rigorous sense. In typical calculations performed in the past, z_T was taken as 225 km, and c_T was taken as the sound speed ($\approx$ 800 m/sec) at that altitude (ref. 8).

The formulation leading to that version of Eq. (1) which is appropriate to infrasound for frequencies at which gravitational effects are important (corresponding to periods greater than one to five minutes) is based on the equations of fluid dynamics with the inclusion of gravitational body forces, the associated nearly exponential decrease of ambient density and pressure with height, and a localized energy source. When c_T is taken to be finite, the incorporation of gravitational effects in this formulation leads to a dispersion relation for plane waves propagating in the upper halfspace which is (winds neglected) (refs. 8,9)

$$k_z^2 = -G^2 = [\omega^2 - \omega_A^2]/c_T^2 - [\omega^2 - \omega_B^2]k^2/\omega^2, \tag{3}$$

where the solution of the linearized equations of fluid dynamics for $z > z_T$ is of the form

$$p/\sqrt{\rho_o} = (\text{Constant})\ e^{-i\omega t}\ e^{ikx}\ e^{ik_z z}. \tag{4}$$

In these equations p is again the acoustic pressure, ρ_o is ambient density, x is the horizontal space dimension, and k_z is the vertical wave number (alternatively written as iG for inhomogeneous plane waves). ω_A and ω_B are two characteristic frequencies ($\omega_A > \omega_B$) for wave propagation in an isothermal atmosphere where $\omega_A = (\gamma/2)g/c_T$ and $\omega_B = (\gamma - 1)^{1/2}\ g/c_T$ ($g \approx 9.8$ m/sec^2 is the acceleration due to gravity and $\gamma \approx 1.4$ is the specific heat ratio for air). The values of k (positive and negative) at which G^2 is zero turn out to be the branch points in the k integration in Eq. (1). The branch lines extend upwards and downwards from the positive and negative branch points, respectively (recall Fig. 1).

The eigenmode dispersion function $D(\omega,k)$ in the case of atmospheric infrasound can be written in the general form (ref. 8)

$$D(\omega,k) = A_{12}R_{11} - A_{11}R_{12} - R_{12}G. \tag{5}$$

In this expression, R_{11} and R_{12} are the elements of a transmission matrix [R]. They depend on the atmospheric properties only in the altitude range zero to z_T, and are independent of what is assumed for the upper halfspace. In general, their determination requires numerical integration over height of two simultaneous ordinary differential equations [termed the residual equations (refs. 8,9,11)]. They do depend on ω and k (or, alternately, on ω and phase velocity $v = \omega/k$), but are free from branch cuts. The other parameters A_{12} and A_{11} depend on the properties of the upper halfspace, and on ω and k. A_{11} and A_{12} are given (winds excluded) as

$$A_{11} = gk^2/\omega^2 - \gamma g/[2c_T^2]; \tag{6a}$$

$$A_{12} = 1 - c_T^2 k^2/\omega^2. \qquad (6b)$$

It may be noted that, since every quantity in Eq. (5) (with the possible exception of G) is real when ω and k are real, the poles that lie on the real k-axis (recall that they are the real roots of D) must be in those regions of the (ω,k)-plane [or, alternatively, the (ω,v)-plane] where $G^2 > 0$. Since at heights above z_T, the integrand of Eq. (1) divided by $\sqrt{\rho_o}$ should vary with z as e^{-Gz_T}, there is no leakage of energy into the upper halfspace for those modes that correspond to the above poles. Such modes are termed fully ducted modes. Modes for which there is leakage of energy are termed leaking. If D is considered as a function of ω and phase velocity v, the locus of its real roots $v(\omega)$ (dispersion curves) has [as has been found by numerical computation with the program INFRASONIC WAVEFORMS (ref. 8)] the general form sketched in Fig. 3. The nomenclature for labeling the modes (GR for gravity, S for sound) is due to Press and Harkrider (ref. 12). It may be noted from Eq. (3) that there are two "forbidden regions" (slashed in the figure) in the (ω,v)-plane. Within these regions there are no real roots of the function $D(\omega,v)$ because G is imaginary. The existence of the high-frequency upper "forbidden region" implies that the phase velocities for propagating modes are always less than the sound speed chosen for the upper halfspace. The low-frequency lower-phase-velocity "forbidden region" appears to be due to the incorporation of gravitational effects into the formulation. However, if c_T is allowed to approach infinity, the lower "forbidden region" disappears. Thus, it can be seen that the fully ducted GR_0 and GR_1 modes both have a low-frequency cutoff [ω_L in Eq. (2)] which depends on c_T. In fact, the larger c_T becomes, the smaller this cutoff frequency becomes.

At this point, there should appear to be the following paradoxes. Given that frequencies below ω_B may be important for the synthesis of a waveform, an apparently plausible computational scheme based on the reasoning leading to Eq. (2) will omit much of the information conveyed by such frequencies. Also, in spite of the plausible premise that energy ducted primarily in the lower atmosphere should be insensitive to the choice for c_T, it can be seen that this choice governs the cutoff frequencies for certain modes and that certain important frequency ranges could conceivably be omitted by a seemingly logical choice for c_T. The resolution of these paradoxes seems to lie in the nature of the approximations made in going from Eq. (1) to Eq. (2). The latter equation may not be as nearly correct as earlier presumed, and it may be necessary to include contributions from poles off the real axis as well as from the branch line integrals. Even for the case when the propagation distance r is very long, it may be that the imaginary parts of the complex horizontal wave numbers are so small that the magnitude of e^{ikr} in Eq. (1) is still not small compared to unity. In addition, a branch line integral may be appreciable in magnitude at large r if there is a pole relatively close to the associated branch cut.

ROOTS OF THE DISPERSION FUNCTION

In light of the paradoxes mentioned, it would be desirable to modify the solution represented by Eq. (2) so as to remove the apparent artificial low-frequency cutoffs of the GR_0 and GR_1 modes. As a first step, the nature of the eigenmode dispersion function D in the vicinity of the dispersion curve for

a particular mode is examined. The curve of values $v_n(\omega)$ of phase velocity v versus ω for a given (n-th) mode is known for frequencies greater than the low cutoff frequency ω_L. Given this curve, analogous curves $v_a(\omega)$ and $v_b(\omega)$ can be found for values of the phase velocity ω/k at which the functions $R_{11}(\omega,v)$ and $R_{12}(\omega,v)$ in Eq. (5), respectively, vanish. One characteristic of the curves $v_n(\omega)$, $v_a(\omega)$, and $v_b(\omega)$ which has been checked numerically for $\omega > \omega_L$ (see Fig. 4) is that, for a given mode of interest, these curves all lie substantially closer to one another than to the corresponding curves for a different mode.

Given the definitions above of $v_a(\omega)$ and $v_b(\omega)$, the dispersion relation $D = 0$ for a single mode may be approximately expressed, through a simple expansion, as

$$D \approx (A_{12})(\alpha)(v - v_a) - [A_{11} + G](\beta)(v - v_b) = 0, \tag{7}$$

where $\alpha = dR_{11}/dv$, and $\beta = dR_{12}/dv$, evaluated at $v = v_a$ and v_b, respectively (for simplicity, D is considered here as a function of ω and $v = \omega/k$ rather than of ω and k). The above equation may also be written in the form

$$v^{(1)} = v_a + (v_a - v_b)X/[1-X], \tag{8a}$$

where

$$X = (\beta/\alpha)(A_{11} + G)/A_{12}. \tag{8b}$$

Eq. (8a) may be considered as a starting point for an iterative solution which develops v in a power series in $v_a - v_b$. With $v = v_a$ as the zeroth iteration, the right hand side of Eq. (8a) can be evaluated for the value of v required for the next iteration, etc. This iterative procedure should converge provided that v_a or v_b is not near a point at which G vanishes and provided that G in the vicinity of v_a or v_b is not such that the variable X is close to unity. Among other limitations, the iterative scheme is inappropriate for those values of ω in the immediate vicinity of ω_L.

As an illustration of the perturbation technique, detailed plots (for the GR_0 and GR_1 modes) versus angular frequency are given in Fig. 5 of ω/k_R (top portion of the figure) which is the reciprocal of the real part of $1/v^{(1)}$, and of k_I (bottom portion) which is the imaginary part of $\omega/v^{(1)}$ (k_R and k_I are the real and imaginary parts of k, respectively), where $v^{(1)}$ is the result of first iteration for the phase velocity using Eqs. (8). Note that k_I is zero above the corresponding cutoff frequencies. The values shown in Fig. 5 are appropriate to the case of a U. S. Standard Atmosphere (ref. 8; see also Fig. 2) without winds which is terminated at a height of 125 km by an upper halfspace possessing a sound speed of 478 m/sec. For frequencies at which v_n is computed, the agreement between $v^{(1)}$ and v_n has proven to be excellent. The ω/k_R serve as approximate extensions of the dispersion curves down to frequencies near zero, thus enabling the computation of waveforms with leaking modes included.

TRANSITION OF MODES FROM NON-LEAKING TO LEAKING

A more precise approximation to $D(\omega,v)$ in the vicinity of cutoff [i.e., near the point (ω_L,v_L)] reveals that a dispersion curve becomes tangential to

the line $G^2 = 0$ at (ω_L, v_L). For $\omega < \omega_L$, there is a very narrow gap in the frequency range in which there are no poles in the k- (or v-) plane corresponding to a given n-th mode. This gap is of the order 10^{-13} rad/sec for the GR_0 mode and 10^{-9} rad/sec for the GR_1 mode.

Since there is a gap in the range of frequencies for which a pole (corresponding to a mode) may exist, it is evident that evaluation of the integral over k in Eq. (1) by merely including residues may be insufficient for certain frequencies. Thus it would seem appropriate to include a contribution from branch line integrals. However, there is a line of reasoning which demonstrates that all contributions from branch line integrals are insignificant as previously assumed. Further details on this matter are provided in reference 13.

EXAMPLE (HOUSATONIC)

Values of ω/k_R and k_I calculated by the perturbation techniques outlined above were used [with a revised version of INFRASONIC WAVEFORMS (ref. 14)] to compute waveforms for the case of signals observed at Berkeley, California, following the Housatonic detonation at Johnson Island on October 30, 1962. A comparison of theoretical and observed waveforms for this case is given by Pierce, Posey, and Iliff (ref. 9). This case also serves as the main example in the 1970 AFCRL report by Pierce and Posey (ref. 8), and is discussed by Posey (ref. 15) within the context of the theory of the Lamb edge mode. The model atmosphere assumed here (winds included) is the same as in Fig. 3-12 of reference 8, except that in the present model the upper halfspace begins at 125 km rather than at 225 km. To avoid repeating tedious calculations of the k_I for the GR_0 and GR_1 modes for this model atmosphere, it was assumed that the k_I would be close in value to those shown in Fig. 5.

In Fig. 6, sets of plots for the Housatonic case are shown with and without leaking modes. The waveform that includes leaking modes is regarded as an improvement in that among other things, the spurious initial pressure drop shown in the original waveform is not present here. In Fig. 7 of reference 9 observed and theoretical waveforms are shown for the Housatonic case. On the basis of the calculations described above, this figure was redrawn and is given here as Fig. 7. The only difference between the two figures lies in the central waveform. The false precursor is absent in the waveform shown in Fig. 7, and the first peak to trough amplitude has been changed from 157 bar to 170 bar (less than a 10% increase). The remainder of the central waveform is virtually unchanged. The discrepancy with the edge-mode synthesis has not been diminished and remains a topic for future study.

CONCLUDING REMARKS

It was shown in this paper that, for a model atmosphere in which the sound speed is constant above some arbitrarily large height, the GR_0 and GR_1 modes have low cutoff frequencies and are leaking below that height. Given these facts, perturbation techniques were provided for the computation of the imaginary and real parts k_I and k_R, respectively, of the horizontal wave numbers for these modes. Knowledge of the k_I and k_R then made it possible to include, in a synthesis of waveforms, contributions from the GR_0 and GR_1 modes at frequencies where these modes were leaking. Finally it was demonstrated that this inclusion yielded waveforms that were more realistic than before.

REFERENCES

1. Thomas, J. E.; Pierce, A. D.; Flinn, E. A.; and Craine, L. B.: "Bibliography on Infrasonic Waves," Geophys. J. R. Astr. Soc. 26, 299-426 (1971).

2. Officer, C. G.: Introduction to the Theory of Sound Transmission with Application to the Ocean (McGraw-Hill, New York, 1958).

3. Wait, J. R.: Electromagnetic Waves in Stratified Media (Pergamon Press, Inc., New York, 1962).

4. Brekhovskikh, L. M.: Waves in Layered Media (Academic Press, New York, 1960).

5. Budden, K. G.: The Wave-Guide Mode Theory of Wave Propagation (Prentice-Hall, Inc., Englewood Cliffs, N. J., 1961).

6. Tolstoy, I. and Clay, C. S.: Ocean Acoustics (McGraw-Hill, New York, 1966).

7. Ewing, M.; Jardetzky, W.; and Press, F.: Elastic Waves in Layered Media (McGraw-Hill, New York, 1957).

8. Pierce, A. D. and Posey, J. W.: Theoretical Prediction of Acoustic-Gravity Pressure Waveforms generated by Large Explosions in the Atmosphere, Report AFCRL-70-0134, Air Force Cambridge Research Laboratories, 1970.

9. Pierce, A. D.; Posey, J. W.; and Iliff, E. F.: "Variation of Nuclear Explosion generated Acoustic-Gravity Waveforms with Burst Height and with Energy Yield," J. Geophys. Res. 76, 5025-5042 (1971).

10. Copson, E. T.: An Introduction to the Theory of Functions of a Complex Variable (Clarendon Press, Oxford, 1935) p. 137.

11. Pierce, A. D.: "The Multilayer Approximation for Infrasonic Wave Propagation in a Temperature and Wind-Stratified Atmosphere," J. Comp. Phys. 1, 343-366 (1967).

12. Press, F. and Harkrider, D.: "Propagation of Acoustic-Gravity Waves in the Atmosphere," J. Geophys. Res. 67, 3889-3908 (1962).

13. Pierce, A. D.; Kinney, W. A.; and Kapper, C. Y.: "Atmosphere Acoustic-Gravity Modes at Frequecies near and below Low Frequency Cutoff Imposed by Upper Boundary Conditions," Report No. AFCRL-TR-75-0639, Air Force Cambridge Research Laboratories, Hanscom AFB, Mass. 01731 (1 March 1976).

14. Pierce, A. D. and Kinney, W. A.: "Computational Techniques for the Study of Infrasound Propagation in the Atmosphere," Report No. AFCL-TR-76-0056, Air Force Geophysics Laboratory, Hanscomb AFB, Mass. 01731 (13 March 1976)

15. Posey, J. W.: "Application of Lamb Edge Mode Theory in the Analysis of Explosively Generated Infrasound," Ph.D. Thesis, Dept. of Mech. Engrg., Mass. Inst. of Tech. (August, 1971).

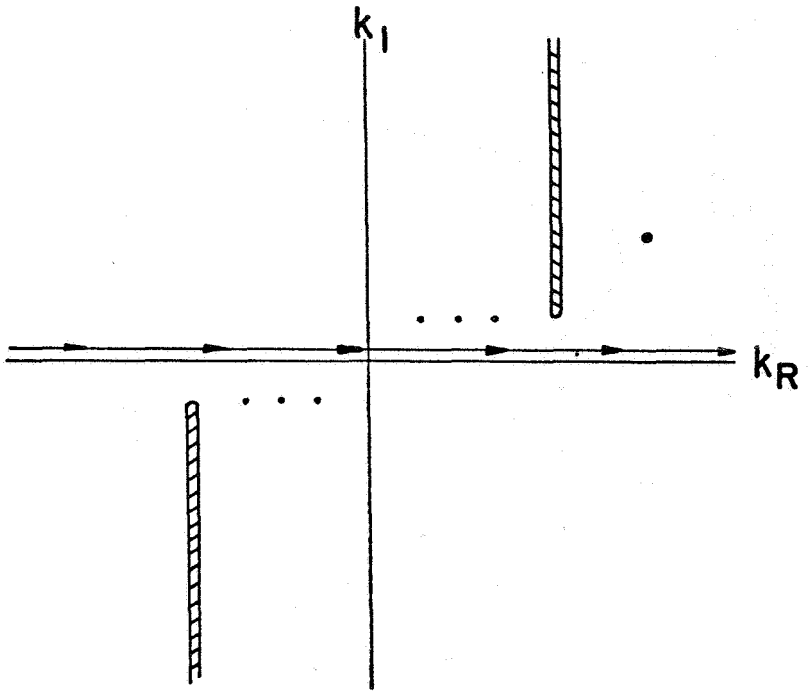

(a) Original.

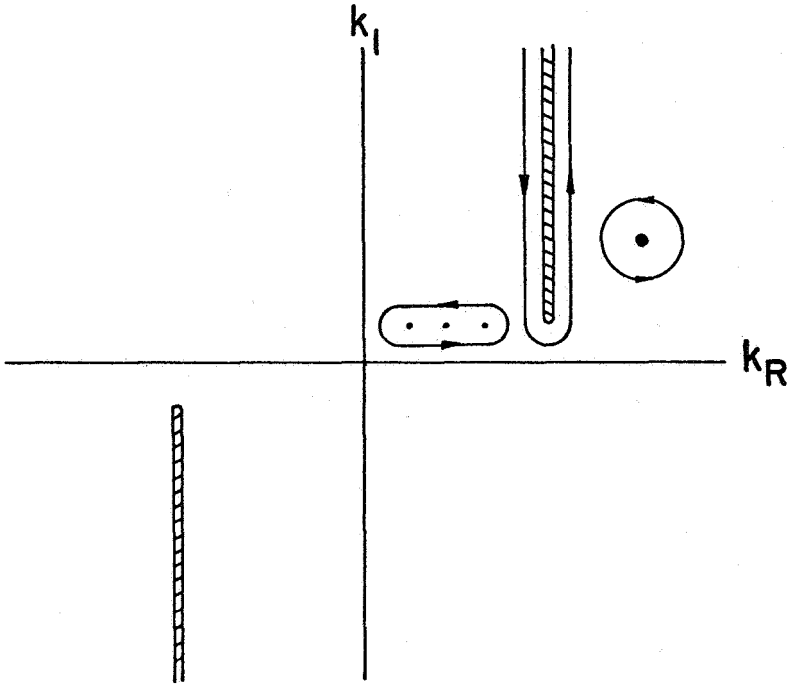

(b) Deformed.

Figure 1.- k-integration contours.

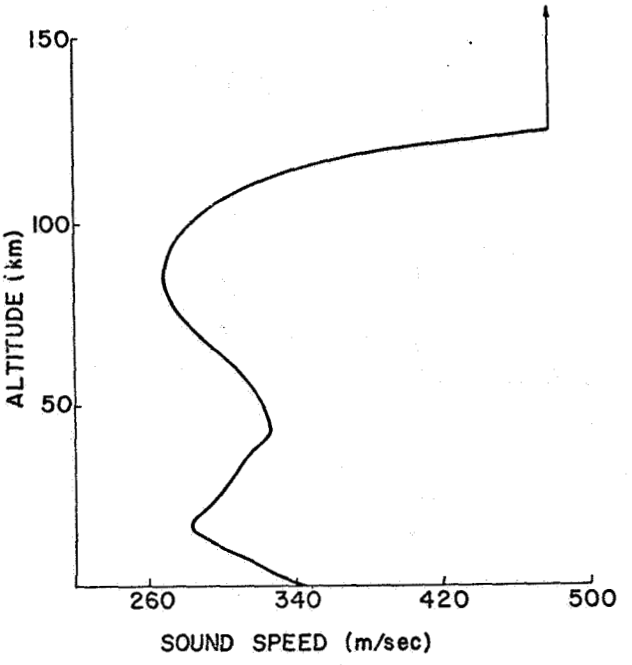

Figure 2.- Model atmosphere.

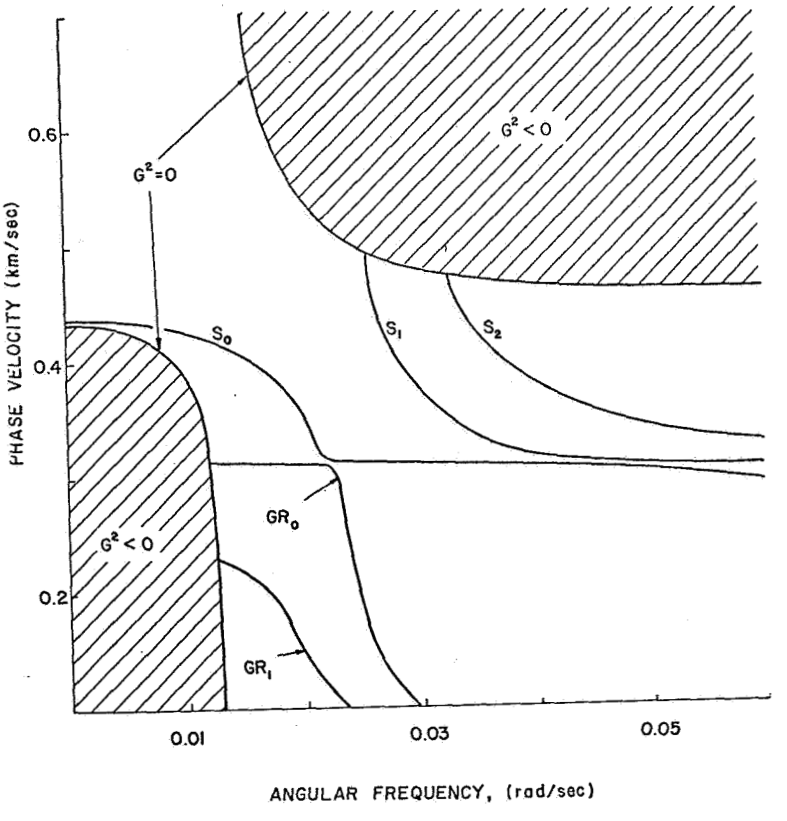

Figure 3.- Dispersion curves.

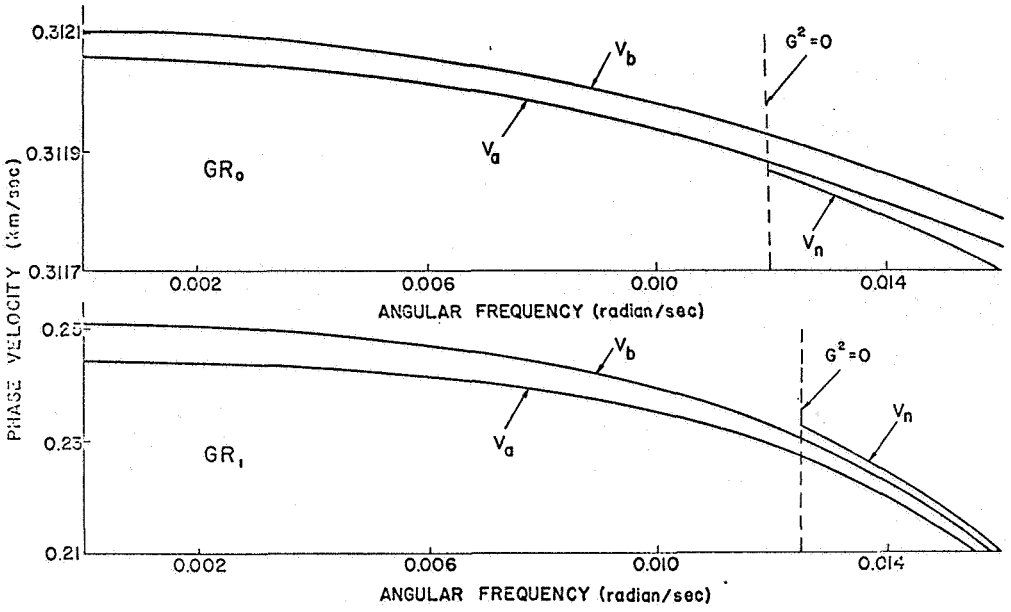

Figure 4.- Curves of v_n, v_a, and v_b.

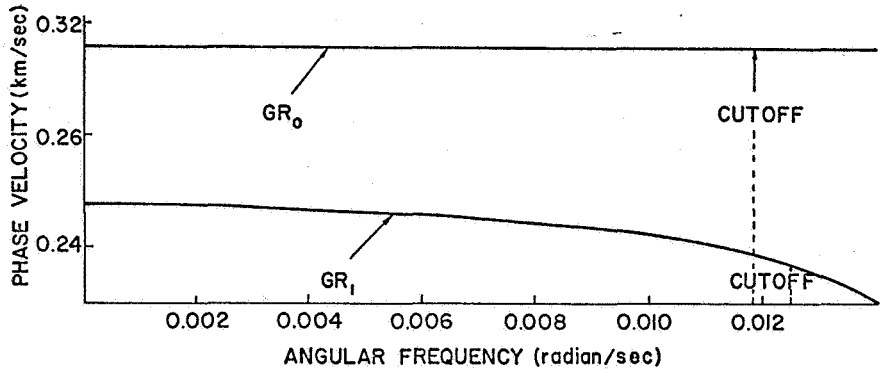

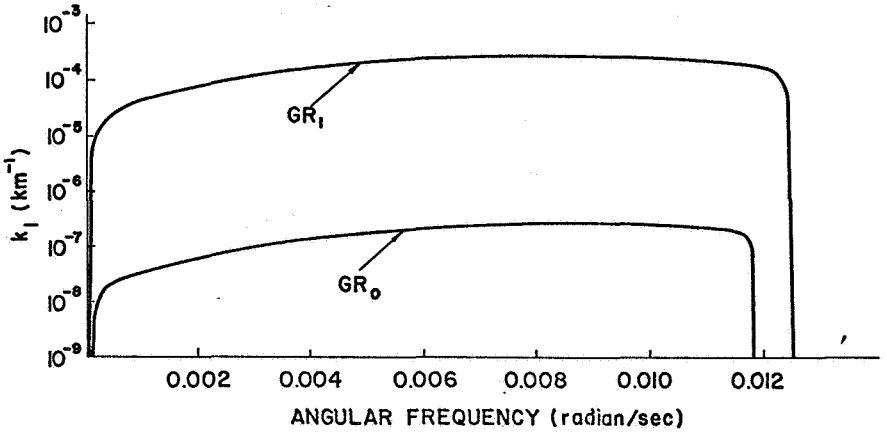

Figure 5.- Curves of ω/k_R and k_I.

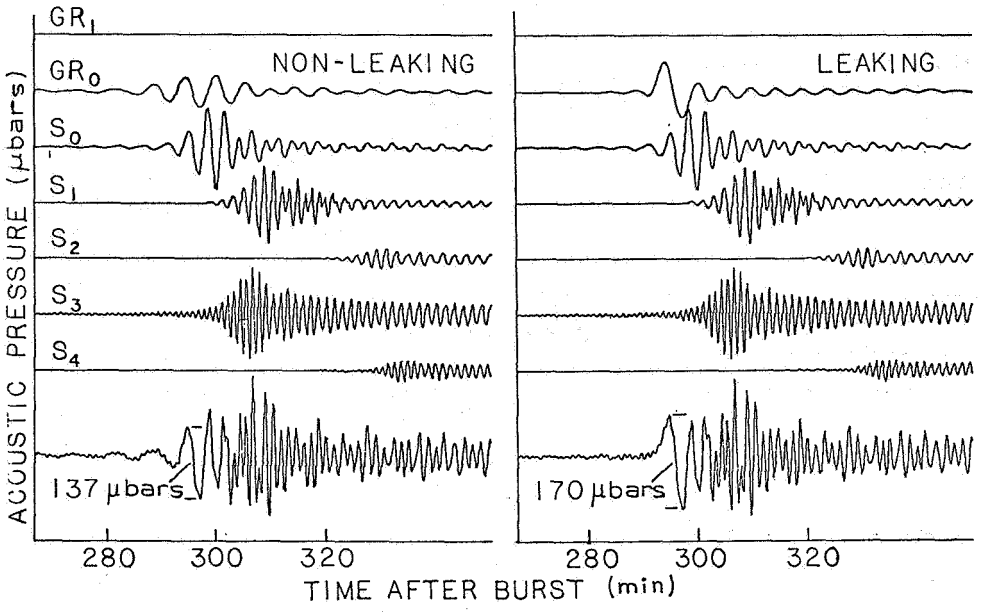

Figure 6.- Numerically synthesized waveforms (Housatonic).

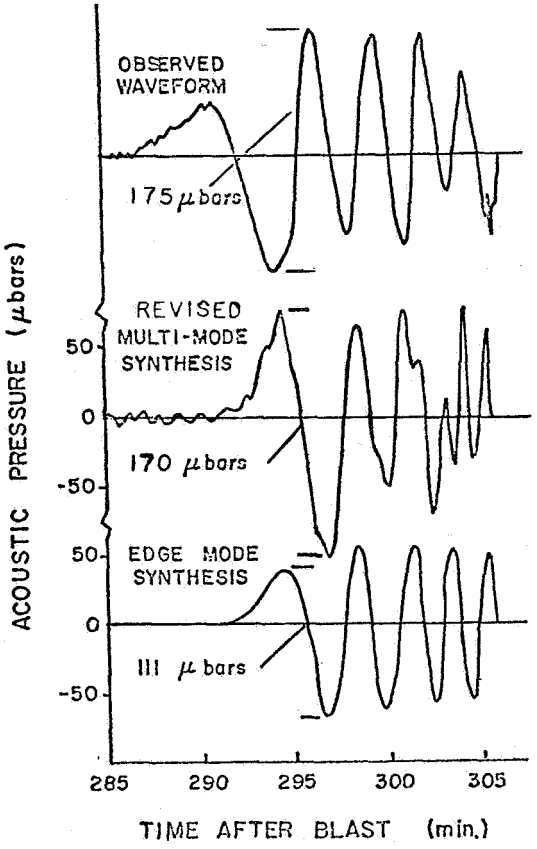

Figure 7.- Observed and theoretical waveforms (Housatonic).